Discovery of a small protein factor involved in the coordinated degradation of phycobilisomes in cyanobacteria

Vanessa Krauspe[a], Matthias Fahrner[b,c,d], Philipp Spät[e], Claudia Steglich[a], Nicole Frankenberg-Dinkel[f], Boris Maček[e], Oliver Schilling[b], and Wolfgang R. Hess[a,1]

[a]Genetics and Experimental Bioinformatics, Faculty of Biology, University of Freiburg, 79104 Freiburg, Germany; [b]Institute for Surgical Pathology, Medical Center–University of Freiburg, Faculty of Medicine, University of Freiburg, 79106 Freiburg, Germany; [c]Faculty of Biology, Albert-Ludwigs University of Freiburg, 79104 Freiburg, Germany; [d]Spemann Graduate School of Biology and Medicine, Albert-Ludwigs University of Freiburg, 79104 Freiburg, Germany; [e]Department of Quantitative Proteomics, Interfaculty Institute for Cell Biology, University of Tübingen, 72076 Tübingen, Germany; and [f]Department of Microbiology, Faculty of Biology, University of Kaiserslautern, 67663 Kaiserslautern, Germany

Edited by Eva-Mari Aro, University of Turku, Turku, Finland, and approved December 17, 2020 (received for review June 18, 2020)

Phycobilisomes are the major pigment–protein antenna complexes that perform photosynthetic light harvesting in cyanobacteria, rhodophyte, and glaucophyte algae. Up to 50% of the cellular nitrogen can be stored in their giant structures. Accordingly, upon nitrogen depletion, phycobilisomes are rapidly degraded following an intricate genetic program. Here, we describe the role of NblD, a cysteine-rich, small protein in this process in cyanobacteria. Deletion of the *nblD* gene in the cyanobacterium *Synechocystis* sp. PCC 6803 prevented the degradation of phycobilisomes, leading to a nonbleaching (*nbl*) phenotype, which could be complemented by a plasmid-localized gene copy. Competitive growth experiments between the Δ*nblD* and the wild-type strain provided direct evidence for the physiological importance of NblD under nitrogen-limited conditions. Ectopic expression of NblD under nitrogen-replete conditions showed no effect, in contrast to the unrelated proteolysis adaptors NblA1 and NblA2, which can trigger phycobilisome degradation. Transcriptome analysis indicated increased *nblA1/2* transcript levels in the Δ*nblD* strain during nitrogen starvation, implying that NblD does not act as a transcriptional (co) regulator. However, immunoprecipitation and far-western experiments identified the chromophorylated (holo form) of the phycocyanin β-subunit (CpcB) as its target, while apo-CpcB was not bound. The addition of recombinant NblD to isolated phycobilisomes caused a reduction in phycocyanin absorbance and a broadening and shifting of the peak to lower wavelengths, indicating the occurrence of structural changes. These data demonstrate that NblD plays a crucial role in the coordinated dismantling of phycobilisomes and add it as a factor to the genetically programmed response to nitrogen starvation.

cyanobacteria | nitrogen starvation | gene expression | photosynthesis | phycobilisomes

The Response of Cyanobacteria to Nitrogen Starvation Is Governed by a Complex Genetic Program

Nitrogen is an essential element of all organisms and frequently the main nutrient limiting life of photoautotrophic primary producers in many terrestrial, freshwater, and marine ecosystems (1, 2). Cyanobacteria are the only prokaryotic primary producers performing oxygenic photosynthesis. Some cyanobacteria are of overwhelming relevance for the global biogeochemical cycles of carbon and nitrogen, exemplified by *Prochlorococcus* and *Synechococcus* with their estimated global mean annual abundances of $2.9 \pm 0.1 \times 10^{27}$ and $7.0 \pm 0.3 \times 10^{26}$ cells (3–5). Other cyanobacteria came into focus for the ease of their genetic manipulation, fast growth, and as platforms for the CO_2-neutral production of diverse valuable products (6, 7). With regard to their response to nitrogen starvation, cyanobacteria can be divided into two major physiological groups. Diazotrophic genera such as *Trichodesmium*, *Nodularia*, *Cyanothece*, *Nostoc*, and *Anabaena* avoid nitrogen limitation by expressing nitrogenase to fix the omnipresent gaseous N_2. In contrast, nondiazotrophic cyanobacteria such as *Synechococcus* and *Synechocystis* stop growth and switch their metabolism from anabolism to maintenance, a process that is controlled by a complex genetic program (8–10). An acute scarcity in the available nitrogen is sensed directly by two central regulators of nitrogen assimilation in cyanobacteria, P_{II} and NtcA, by binding the key metabolite 2-oxoglutarate (2-OG) (11–15). 2-OG is the substrate for amination by glutamine oxoglutarate aminotransferase, which catalyzes the transfer of the amino group from glutamine to 2-OG, yielding two molecules of glutamate. This glutamate then is the substrate for amination by glutamine synthetase, the central enzyme of nitrogen assimilation in cyanobacteria. As a consequence, the intracellular level of 2-OG starts to increase once these reactions slow down due to insufficient nitrogen supply, making 2-OG an excellent indicator of nitrogen status (16). Binding of 2-OG stimulates the activity of NtcA, the main transcriptional regulator of nitrogen assimilation (11, 12). Depending on the 2-OG level, PipX switches from binding to P_{II}

Significance

During genome analysis, genes encoding small proteins are frequently neglected. Accordingly, small proteins have remained underinvestigated in all domains of life. Based on a previous systematic search for such genes, we present the functional analysis of the 66 amino acids protein NblD in a photosynthetic cyanobacterium. We show that NblD plays a crucial role during the coordinated dismantling of phycobilisome light-harvesting complexes. This disassembly is triggered when the cells become starved for nitrogen, a condition that frequently occurs in nature. Similar to NblA that tags phycobiliproteins for proteolysis, NblD binds to phycocyanin polypeptides but has a different function. The results show that, even in a well-investigated process, crucial new players can be discovered if small proteins are taken into consideration.

Author contributions: W.R.H. designed research; V.K., M.F., P.S., and W.R.H. performed research; V.K., M.F., P.S., C.S., N.F.-D., B.M., O.S., and W.R.H. analyzed data; and V.K. and W.R.H. wrote the paper.

The authors declare no competing interest.

This article is a PNAS Direct Submission.

[1]To whom correspondence may be addressed. Email: wolfgang.hess@biologie.uni-freiburg.de.

This article contains supporting information online at https://www.pnas.org/lookup/suppl/doi:10.1073/pnas.2012277118/-/DCSupplemental.

Published January 28, 2021.

to interacting with NtcA, further enhancing the binding affinity of this complex to target promoters (13, 15). In the model cyanobacterium *Synechocystis* sp. PCC 6803 (*Synechocystis* 6803), NtcA directly activates 51 genes and represses 28 other genes after 4 h of nitrogen starvation (17). Among the NtcA-activated genes are the cotranscribed genes *nblA1* and *nblA2* (*ssl0452* and *ssl0453*) (17). Once they are expressed, NblA proteins impact the physiology dramatically. They initiate the degradation of phycobiliproteins, the major light-harvesting pigments in the cyanobacterial phycobilisomes, a process that is visible by the naked eye as chlorosis (18, 19).

Phycobilisomes, the Most Efficient Structures for Photosynthetic Light Harvesting, Become Degraded during Nitrogen Starvation

Phycobilisomes are the major light-harvesting system in red algae and most cyanobacteria (20). Phycobilisomes are giant protein–pigment complexes anchored to the thylakoid membranes (21, 22) that absorb light mainly in the "green gap" between 580 and 650 nm. Phycobilisomes consist of light-absorbing phycobiliproteins (in *Synechocystis* 6803 phycocyanin [PC] and allophycocyanin [APC]) carrying open-chain tetrapyrroles as chromophores and of structurally important linker proteins. Phycobilisome complexes are highly abundant and may contain up to 50% of the soluble cellular protein and nitrogen content (23). Therefore, their ordered disassembly is part of the physiological response to nitrogen starvation (10, 18, 19, 24, 25) that can free a substantial amount of amino acids (aa) and release the nitrogen bound as part of the photosynthetic pigment molecules.

The degradation of phycobiliproteins is initiated by NblA proteins. Mutations in the *nonbleaching* A (*nblA*) genes yield, unlike the wild-type strain, a nonbleaching phenotype under nitrogen starvation because they do not degrade their phycobilisomes (26–28). Binding experiments indicated that NblA likely interacts with the α-subunits of phycobiliproteins in *Tolypothrix* PCC 7601 (29) and *Anabaena* sp. PCC 7120 (30); however, in *Synechococcus elongatus* UTEX 2973, it was found to bind to the N terminus of the PC β subunit (CpcB) (31). Pull-down experiments then led to the discovery that NblA acts as an adaptor protein for the Clp protease by also interacting with the ClpC chaperone (32). Because the chaperone partner determines the substrate specificity of this protease, NblA presents the protein components of the phycobilisome for proteolysis. The extensive characterization of additional mutants with an *nbl* phenotype in *Synechococcus elongatus* PCC 7942 (*S. elongatus* 7942) led to the discovery of further enzymes and regulatory proteins, NblB1, NblB2, NblC, NblR, and NblS, which play roles in the preprogrammed disassembly of phycobilisomes during nitrogen starvation (Table 1).

In contrast to these observations in *S. elongatus* 7942, the mutations of corresponding genes in *Synechocystis* 6803, Δ*slr1687* (NblB homolog #2), Δ*sll0396* (NblR homolog), and Δ*sll0698* (NblS homolog) did not yield a nonbleaching phenotype during nitrogen depletion (33, 34). These findings suggest that, in addition to commonalities, substantial differences exist in the response of certain species to nitrogen depletion and the organization of the photosynthetic apparatus. Nevertheless, the acclimation of nondiazotrophic cyanobacteria to nitrogen starvation and the process leading to the ordered degradation of phycobilisomes and phycobiliproteins is considered to be governed by a hierarchically structured intricate genetic program (10, 25).

Small Proteins in Cyanobacteria

The aforementioned proteolysis adaptors NblA1 and NblA2 are small proteins of just 62 and 60 residues, respectively. During standard genome analyses, small open reading frames (smORFs) encoding such proteins shorter than 70 aa are frequently neglected. The identification of small proteins by mass spectrometry (MS) based on shotgun proteomics is also difficult. According to their length, these proteins contain only a few or even miss cleavage sites for commonly used proteases such as trypsin. Consequently, the number of generated peptides is smaller than that for larger proteins. Additionally, MS spectra with only a few unique peptides might not fulfill common quality criteria and are removed during filtering. Thus, the number of genes encoding small proteins has been systematically underestimated. In strong contrast is the finding that genes encoding small proteins constitute an essential genomic component in bacteria (35). Recent ribosome profiling studies in bacteria using the inhibitor of translation retapamulin suggest that a high number of previously unexplored small proteins exists in bacteria (36, 37). Detailed analyses are required to identify their functions at the molecular level.

Cyanobacteria provide a paradigm for small protein functions also in addition to the known NblA functions. Extensive work on the photosynthetic apparatus led to the functional characterization of 19 small proteins with fewer than 50 aa. These proteins play indispensable roles in photosystem II [genes *psbM*, *psbT* (*ycf8*), *psbI*, *psbL*, *psbJ*, *psbY*, *psbX*, *psb30* (*ycf12*), *psbN*, *psbF*, and *psbK* (38, 39)], photosystem I [*psaM*, *psaJ*, and *psaI* (40)], photosynthetic electron transport [Cytb_6f complex; *petL*, *petN*, *petM*, and *petG* (41–43)], and photosynthetic complex I [*ndhP* and *ndhQ* (44)] or have accessory functions [*hliC* (*scpB*) (45)]. The shortest annotated photosynthetic protein conserved in cyanobacteria consists of 29 aa—the cytochrome b_6f complex subunit VIII, encoded by *petN* (46).

We have previously analyzed the primary transcriptomes of the model cyanobacterium *Synechocystis* 6803 and the closely related strain *Synechocystis* sp. PCC 6714 (47–49). Based on these analyses, several smORFs likely encoding previously

Table 1. Proteins previously identified in different cyanobacteria as involved in the programmed phycobilisome disassembly and their homologs in *Synechocystis* 6803

Protein name	Gene ID	Function	Reference
NblA1	ssl0452	Protease adaptor	33
NblA2	ssl0453	Protease adaptor	33
ClpC	sll0020	HSP100 chaperone partner of Clp protease	76
NblB1	sll1663	Bilin lyase homolog	33, 64
NblB2	slr1687	Bilin lyase homolog	33, 64
NblC	sll1968	Regulator	87
NblR	sll0396	Regulator	27
GntR	sll1961	Regulator	72
Hik33/NblS/DspA	sll0698	Sensor kinase	34, 88
RpaB/Ycf27	slr0947	Response regulator	89

Synonymous protein names are separated by a slash.

unknown small proteins were computationally predicted. Experiments using a small 3xFLAG epitope tag fused in-frame to the second-to-last codon of the smORF under control of their native promoters and 5′ untranslated regions (UTRs) validated five of these smORFs to encode small proteins (50).

Here, we analyzed one of these small proteins, the 66-residue NsiR6 (nitrogen stress-induced RNA 6), which is highly upregulated following nitrogen removal (47, 50). We show that this small protein is a crucial factor in the genetically programmed response to nitrogen starvation executing a previously unrecognized role in the coordinated disassembly of phycobilisomes. Based on the observed *nbl* phenotype, we renamed NsiR6 to NblD.

Results

Homologs of *nblD* Are Widely Conserved within the Cyanobacterial Phylum. The *nblD* gene in *Synechocystis* 6803 is located on the chromosome, between the genes *slr1704* encoding a hypothetical surface-layer protein and *sll1575* encoding the serine–threonine protein kinase SpkA (51), at a distance of less than 2.5 kb from the *cpcBAC2C1D* operon encoding phycobilisome proteins (Fig. 1*A*). Database searches identified 176 homologs of *nblD* in species belonging to all morphological subsections (52) except section V (*Fischerella* and other cyanobacteria featuring filaments with a branching morphology). Homologous genes were also detected in the three available chromatophore genomes of photosynthetic *Paulinella* species (53). The endosymbiont chromatophore genomes have been reduced to about one-third the size of the genome of its closest free-living relatives (54). Hence, the presence of *nblD* homologs in chromatophore genomes indicates a possible important function connected to the metabolic pathways retained in these organisms. We detected putative homologs also in two diatom-associated symbionts, *Calothrix rhizosoleniae* and *Richelia intracellularis*. However, we found no homologs in the genomes of "Candidatus Atelocyanobacterium thalassa" endosymbionts, which have the capacity for nitrogen fixation but lack photosystem II and phycobilisomes (55, 56), and in the well-studied model *S. elongatus* 7942. Homologs of NblD are also lacking in the genera *Prochlorococcus* and most *Acaryochloris*, which use alternative light-harvesting mechanisms. We noticed, however, the presence of a homolog in *Acaryochloris thomasi* RCC1774, an isolate with a very different pigmentation (57).

The lengths of the 176 homologs identified in this work (Dataset S1) vary between 41 aa in *Crocosphaera watsonii* WH 0005 and 121 aa in *Phormidesmis priestleyi* Ana. The alignment of selected NblD homologs highlights the presence of four conserved cysteine residues (Fig. 1*B*). Moreover, these four cysteine residues are conserved also in all other detected homologs except in seven very short forms, which lack the first cysteine pair (Dataset S1). The first pair of cysteines is arranged in a CPxCG-like motif, typical for zinc-finger structures in small proteins of bacteria and archaea (58, 59). These structures can bind metal ions and initiate loop formation, which is relevant for transcription factors. Additionally, protein–protein interaction conditioned by sulfur bonds between two cysteines is possible. To test this, we used two strains overexpressing NblD fused to a C-terminal 3xFLAG tag, one under the control of its native P_{nblD} promoter and the other under the control of the copper-inducible P_{petE} promoter on plasmid pVZ322, yielding strains P_{nblD}_*nblD*_3×FLAG and P_{petE}_*nblD*_3×FLAG (50). When analyzing total protein extracts from these strains by Western blot analyses, we noticed a second band of higher molecular mass under nonreducing conditions but not in the presence of dithiothreitol (DTT) and β-mercaptoethanol (Fig. 1*C*). This result supported interaction, either as a homodimer or with another partner. Consistent with this result, the prediction tool SWISS MODEL (60) modeled NblD as a homodimer and predicted a helical segment in the most conserved part of the protein (Fig. 1*D*).

We conclude that *nblD* genes exist in a wide range of cyanobacteria and in chromatophore genomes of photosynthetic *Paulinella*, that the NblD protein can form dimers and might interact with other biomolecules, and that a regulatory role cannot be excluded.

Transcriptomic Analysis Identifies a Functional Response to Nitrogen Step-Down in the Δ*nblD* Mutant. To identify possible effects on the regulation of gene expression, the *nblD* gene was replaced by a kanamycin resistance cassette. Putative transconjugants were

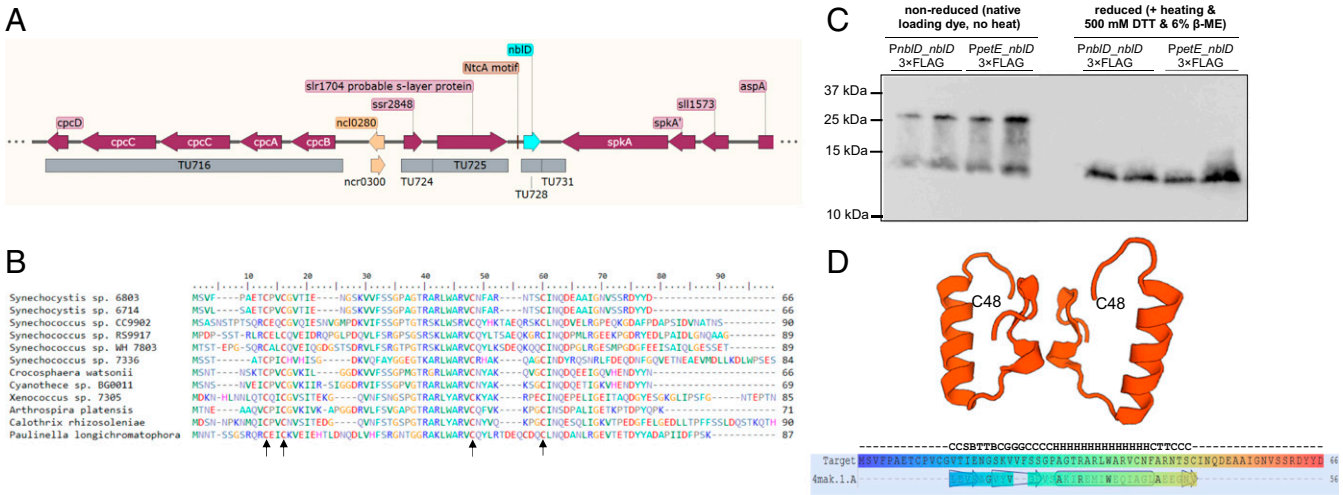

Fig. 1. (*A*) Genomic location of *nblD* in *Synechocystis* 6803. TUs are indicated according to the previous annotation of the transcriptome and genome-wide mapping of transcriptional start sites (47). (*B*) Alignment of NblD homologs from cyanobacteria belonging to four morphological subsections (52); conserved cysteine residues are marked by an arrow. (*C*) Western blotting using anti-FLAG antiserum against tagged NblD and reducing and nonreducing conditions for SDS-PAGE. The expression of *nblD* was induced by nitrogen removal (native P_{nblD} promoter) or the addition of 2 μM Cu^{2+} ions (P_{petE} promoter). All samples were loaded in biological duplicates. (*D*) Predicted NblD structure generated by SWISS-MODEL (60) as a homodimer using the crystal structure of the *E. coli* Cas2 CRISPR protein 4mak.1 as template. The structure is modeled from position 14A to C48; the position of the latter in the two molecules is given for orientation. (*Lower*) Alignment of NblD (Target) to template; the sequence is rainbow colored from blue (N terminus) to red (C terminus). The symbols indicate predicted secondary structure (G = three-turn helix, H = α helix, T = hydrogen-bonded turn, B = residue in isolated β-bridge, S = bend, and C = coil).

restreaked to allow segregation of wild-type and mutant alleles of *nblD* (*SI Appendix*, Fig. S1). Total RNA was isolated from Δ*nblD* and the wild-type immediately before (0 h) and 3 h after nitrogen removal to evaluate possible direct effects of NblD on transcription. For the genome-wide assessment of steady-state RNA levels, high-density microarrays were used that employ probes for all 8,916 previously detected transcripts originating from loci on the chromosome or seven plasmids (47, 49). The array design allows the direct hybridization of total RNA, avoiding the pitfalls of complementary DNA synthesis. As expected, the lack of *nblD* transcription was readily detected in the microarray, indicated by a $\log_2$ fold change (FC) of −4.5 in the direct comparison between the expression in the wild-type and Δ*nblD* after 3 h of nitrogen deprivation (*SI Appendix*, Table S1). We performed northern hybridizations to verify the transcriptomic data. While no signal was detected in Δ*nblD* confirming the completeness of gene deletion, the *nblD* messenger RNA (mRNA) was detectable in the wild-type 3 h after nitrogen removal and further increasing after 6 h, yielding a single band of ~500 nt (Fig. 2*A*). This matches the sum of the previously calculated lengths of transcriptional unit (TU) 728 and TU731 together, extending from position 729645 to 730159 on the forward strand (GenBank accession no. NC_000911) (47). Hence, a transcript with a maximum length of 514 nt contains the 198 nt *nblD* reading frame positioned from nt 729671 to 729871 (including the stop codon). These data yield a 5′UTR of 26 nt and a 3′UTR of 288 nt for *nblD*. The visualization of microarray data at single-probe resolution shows the absence of signals in Δ*nblD* under any condition, a very low transcript level in the wild-type under nitrogen-replete conditions that was below the sensitivity threshold of the northern hybridization, and an increased transcript level of the downstream-located TU731 in Δ*nblD* under nitrogen starvation (Fig. 2*B*).

Our transcriptomic analysis showed that typical marker genes that normally show increased transcript levels upon nitrogen step-down were detected also in Δ*nblD* (*SI Appendix*, Table S1). For example, the expression of *glnB* encoding the universal nitrogen regulatory protein PII (15, 61) was increased after 3 h of nitrogen starvation in Δ*nblD* by a $\log_2$FC of 2.5 and in wild-type by 2.0 (*SI Appendix*, Table S1). NsiR4, a regulatory small RNA that is under NtcA control (62), showed a very similar gene expression change in the mutant and in the control. The most

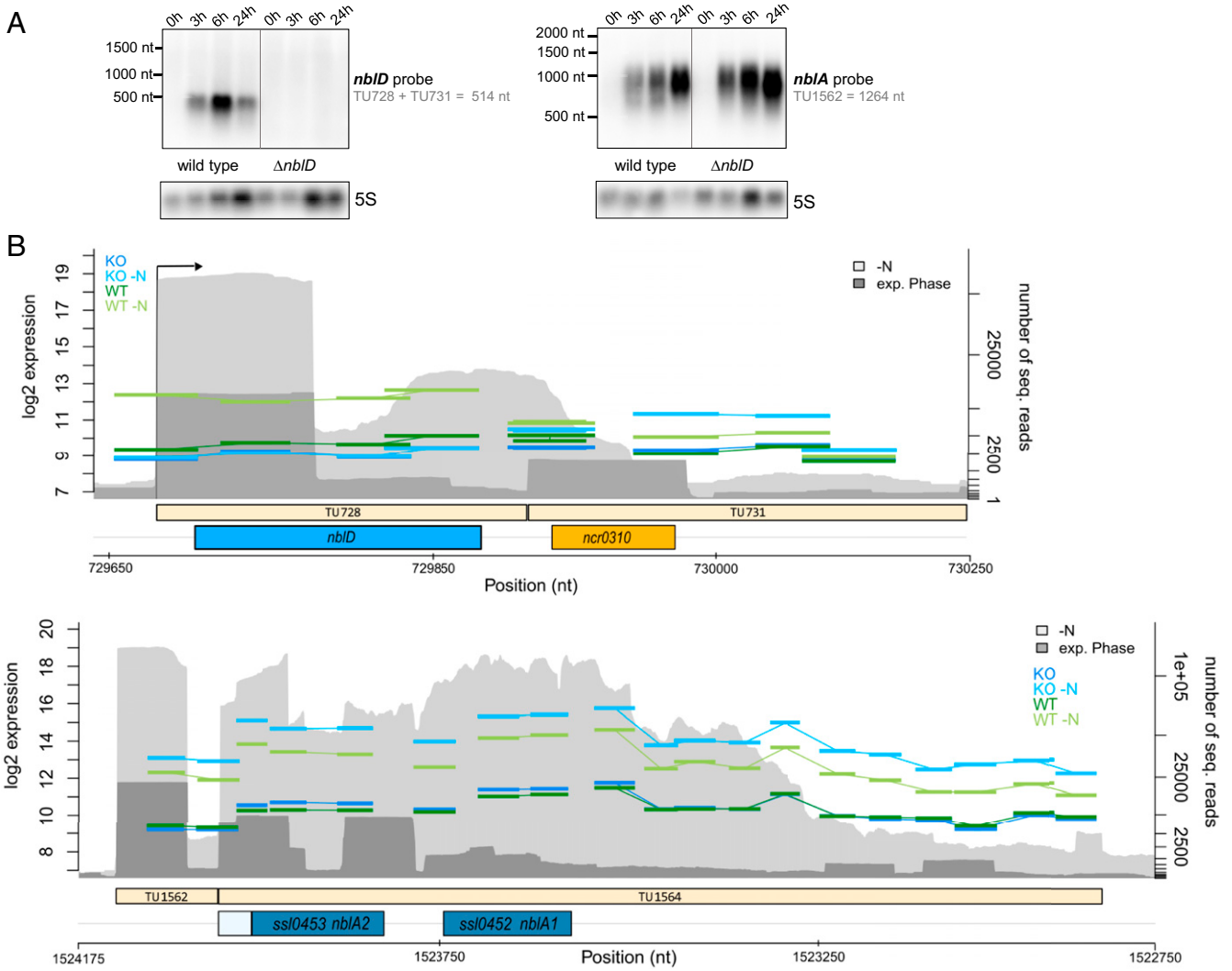

Fig. 2. Changes in the abundance of mRNAs in response to an altered nitrogen supply in wild-type (WT) and Δ*nblD*. (*A*) Northern blot probing *nblD* and *nblA* in the WT and Δ*nblD* mutant at 0, 3, 6, and 24 h after nitrogen removal. (*B*) Microarray data visualized for the TUs for *nblA* (TU1564) and *nblD* (TU728 + TU731). The $\log_2$ expression values of probes were compared for samples from biological duplicates of each WT and Δ*nblD* (KO) cultures grown with nitrogen (dark green and dark blue, respectively) and 3 h after nitrogen removal (-N, lighter green and lighter blue) at the left scale. The number of sequenced reads (47) for the exponential phase (exp. phase, dark gray) and nitrogen starvation for 12 h (-N, light gray) were included in the background (right scale).

strongly increased mRNA levels in the wild-type and Δ*nblD* were found for *nblA1* and *nblA2* with $\log_2$FCs of 3.5/3.7 and 4.1/4.3, respectively, which is consistent with previous reports (28). We noticed slightly higher *nblA1A2* mRNA levels in Δ*nblD* than in the control. This effect, as well as the temporally correct and strongly increased mRNA levels in the deletion mutant, was verified by northern analysis (Fig. 2*A*). The detected signal matches approximately the maximum length of the dicistronic *nblA1A2* transcript TU1564 of 1,264 nt (47). Similar to our observation for *nblD*, this transcript is much longer than that needed to encode the small NblA proteins of 60 and 62 aa, and this extra length mainly belongs to a very long 3′UTR (Fig. 2*B*).

Some genes, such as *gifA* and *gifB*, both encoding inhibitory factors of glutamine synthetase type I, are strongly repressed upon nitrogen step-down (63). Here, we observed a $\log_2$FC of −4.7 in Δ*nblD* and −2.4 in the control, both for *gifA* and *gifB* (*SI Appendix*, Table S1). Hence, also the reduction in the expression of certain genes in the absence of nitrogen was fully operational in the mutant. Moreover, the amplitudes of expression changes were even stronger in Δ*nblD* than in the wild type, pointing at a possibly more pronounced nitrogen starvation effect in the mutant.

In addition to these marker genes for the short-term response to low nitrogen, we observed a small number of further expression changes, mainly in genes related to pigment biosynthesis or storage, such as *hemF*, *nblB1*, *nblB2*, *hliA*, *hliB*, and *hliC* (*SI Appendix*, Table S1 and Fig. S2).

Based on transcriptomic analysis, we conclude that the signaling of nitrogen deficiency through the NtcA and PII-PipX systems must have been fully functional in the Δ*nblD* mutant. Hence, the possibility that NblD acted as a regulator or coregulator of their expression could be excluded. A genome-wide graphical overview of probe localization and the corresponding signal intensities for the wild type and Δ*nblD* mutant just before and 3 h following the shift to nitrogen starvation conditions is available in Dataset S2 and at https://figshare.com/s/308ee7d284599fb2f085. Additionally, the entire dataset can be accessed in the Gene Expression Omnibus database under the accession number GSE149511.

Deletion of *nblD* Causes a Nonbleaching Phenotype during Nitrogen Starvation. To identify a possible phenotype associated with NblD, the Δ*nblD* strain was analyzed. Like the wild type, the mutant showed linear growth under nutrient-replete conditions (*SI Appendix*, Fig. S3), but the phenotypes differed strikingly under nitrogen starvation. The bleaching process was slower and less intense than that of the wild type. Using a complementation plasmid reintroducing an *nblD* gene copy under the control of its native promoter, the wild-type appearance was restored (Fig. 3*A*). Hence, the phenotype of the deletion mutant could be successfully rescued by complementation and the nonbleaching phenotype observed in Δ*nblD* was due to the lack of NblD.

Because we could rule out a role of NblD as a transcription factor, we considered its function as a proteolysis adaptor for the phycobilisome, possibly analogous to NblA. However, ectopic overexpression of *nblD* under the control of the copper-inducible P_{petE} promoter did not cause bleaching (Fig. 3*A*) in nitrogen-replete conditions, different from the effect of *nblA* overexpression in *S. elongatus* 7942 (64). Therefore, NblD cannot initiate the degradation of PC alone, distinguishing it from the activity of NblA, which is a proteolysis adapter protein (32).

By replacing the first two cysteines by serine residues (mutations C9S and C12S) we interrupted the first of two cysteine motifs in NblD. Introduction of this construct on a conjugative vector into Δ*nblD* led to only partial complementation, indicating some functional relevance of this first cysteine motif but no absolute requirement for it. Furthermore, an introduced premature stop codon replacing the second aa (serine) resulted in a nonbleaching phenotype, indicating that the presence of the translated NblD protein is required for the normal phenotype and not a theoretically possible regulatory feature of the transcript. Moreover, we concluded that the presence of the C-terminal triple FLAG tag did not interfere with the physiological function of NblD because complementation with a FLAG-tagged version of NblD was used to restore the wild-type appearance (Fig. 3*A*).

Consistent with the visual inspection, the different absorption around 630 nm in spectra taken after 48 h of nitrogen starvation indicated that photosynthetic pigments, especially phycobiliproteins, were still present in the nonbleaching mutants, while these were almost undetectable in wild-type and complementation lines (Fig. 3*B*). This difference was even more obvious when the data were normalized to the local minimum at 670 nm (Fig. 3*C*). The almost unaffected presence of PC in Δ*nblD* was confirmed in 77 K emission spectra. We used an excitation wavelength of 580 nm, which excites one of the phycocyanobilin chromophores of the CpcB subunit of PC, and normalized to the photosystem I emission maximum at 720 nm. The emission peak at 660 nm (overlapping peaks of bulk PC at ∼652 nm and APC at 665 nm) persisted in Δ*nblD* at a high level in the nitrogen starvation condition. Furthermore, this peak was shifted in Δ*nblD* by 2 nm to shorter wavelengths, indicating a different APC–PC ratio in favor of PC emission. A minor peak at ∼640 nm indicated the presence of small amounts of uncoupled PC, either trimeric or hexameric discs, in the wild-type. This peak was not detectable in wild-type in the nitrogen-replete condition and in Δ*nblD* in neither condition. In comparison, the 680-nm peak, which is caused by fluorescence emitted by photosystem II and the terminal emitters ApcD and ApcE, was reduced under nitrogen starvation in Δ*nblD* similar to the wild-type (Fig. 3*D*).

The high amounts of PC remaining in Δ*nblD* during nitrogen starvation were present in intact phycobilisomes, because these could be isolated 24 h after nitrogen removal, whereas wild-type phycobilisomes were already partly dismantled at this time (*SI Appendix*, Fig. S4). Taken together, the results indicate a role of NblD in the nitrogen starvation–induced physiological program for the degradation of phycobilisomes during the acclimation to nitrogen starvation.

NblD Interacts with CpcB. To obtain insight into the molecular mechanism in which NblD is involved, pull-down experiments were performed. The previously constructed *Synechocystis* 6803 P_{nblD}_*nblD*_3×FLAG line (50) was used to produce FLAG-tagged NblD fusion protein from a plasmid pVZ322-located gene copy under the control of the native promoter. Three hours after nitrogen removal, NblD–FLAG and bound interaction partners were immunoprecipitated from the lysate using anti-FLAG resin and were analyzed by MS (Table 2). After the final wash step, the resulting sample was still bound to the M2-anti-flag–resin, showing a dramatic variation in color. While the control samples appeared color-less, the samples containing the NblD–FLAG lysate kept a strong blue color, indicating the presence of likely nondegraded PC (Fig. 4*A*).

Despite its small size, between seven and nine of nine total unique peptides of NblD were detected in these samples by MS analysis. Furthermore, it was highly abundant according to iBAQ values (65), which corresponds to the total of all the peptide intensities divided by the number of observable peptides of a protein. The detection of NblD at this early time point, only 3 h after transfer to the low nitrogen condition, was consistent with and extended our observation of high-*nblD* mRNA levels at this time (Fig. 2). By contrast, NblD was not detectable in the Δ*nblD* mutant strain. Statistical analysis showed that CpcA and CpcB were the only specifically enriched proteins that coimmunoprecipitated with the NblD–FLAG protein (Fig. 4 *B* and *C*).

To verify the interaction proposed by the results of the MS analysis, we used recombinant NblD fused to a small ubiquitin-related modifier (SUMO)–6×His tag at its N terminus in a far Western

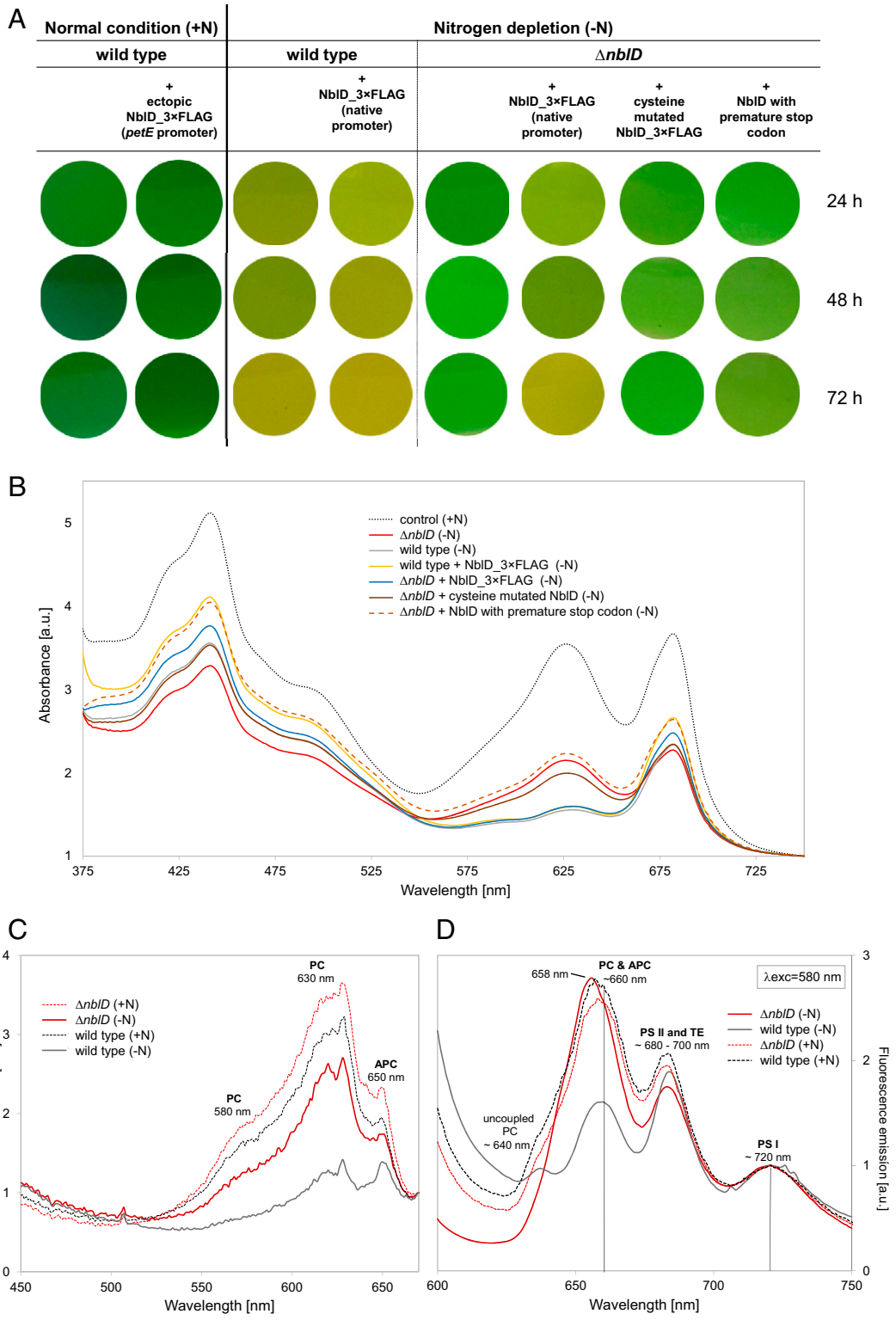

Fig. 3. Phenotypical differences between *nblD* mutants and the wild-type in nitrogen-replete and -deplete media. (*A*) Representative appearance of cultures. (*B*) Room temperature absorbance spectra for *nblD* mutants and wild-type in the presence (control +N) or absence of combined nitrogen for 48 h, normalized to OD_{750}. (*C*) Low-temperature excitation spectra at 77 K for Δ*nblD* and wild-type cultures with and without nitrogen monitored at 690-nm fluorescence emission. The spectra were normalized to the minimum at 670 nm. Characteristic phenotypes of wild-type and mutant with and without nitrogen were measured five times (technical replicates) and averaged. (*D*) Low-temperature 77 K emission spectra at 580 nm excitation for the Δ*nblD* and wild-type strains with and without nitrogen. Samples were measured three times each and averaged. The spectra were normalized to the photosystem I peak at 720 nm. PC, phycocyanin; APC, allophycocyanin; PSI and PSII, photosystem I and II; TE, terminal emitter.

Table 2. Most abundant proteins identified by MS analysis for FLAG affinity–pull-down samples containing tagged NblD versus Δ*nblD* samples and their calculated LFQ intensities (83) using MaxQuant

				Δ*nblD*			nblD_ 3×FLAG		
Protein ID	GO term	MW	aa	1	2	3	1	2	3
Sll1577 CpcB	PS antenna	18.1	172	4.3E + 08	3.6E + 08	2.8E + 08	1.0E + 10	1.2E + 10	7.2E + 09
NblD_3×FLAG fusion protein	n/a	99.3	89	0	0	0	5.2E + 09	7.4E + 09	8.8E + 09
Sll1578 CpcA	PS antenna	17.6	162	5.1E + 08	2.7E + 08	2.9E + 08	4.2E + 09	5.0E + 09	5.5E + 09
Slr0335 PBS core-membrane linker ApcE	PS antenna	100.3	896	2.3E + 09	4.2E + 09	5.5E + 08	2.0E + 09	1.7E + 07	1.3E + 07
Slr1140 DegT/DnrJ/ EryC1/StrS-family protein	Polysa-ccharide synthesis	41.6	378	1.3E + 09	9.8E + 08	2.2E + 09	5.3E + 08	9.1E + 08	6.7E + 08
Sll1580 PBS rod linker CpcC1	PS antenna	32.5	291	1.1E + 09	3.0E + 08	3.2E + 08	8.9E + 08	1.1E + 08	3.1E + 08
Slr2067 ApcA	PS antenna	17.4	161	3.4E + 08	1.4E + 08	1.6E + 08	3.5E + 08	8.9E + 07	8.2E + 07
Ssr0482 30S ribosomal r-protein S16	Ribosome	95.6	82	4.0E + 07	1.7E + 08	3.0E + 08	8.7E + 07	1.1E + 08	2.7E + 08
Sll1099 elongation factor Tu	Translation	43.7	399	4.3E + 08	6.5E + 07	1.2E + 07	2.3E + 08	4.0E + 07	1.3E + 07
Sll1744 50S ribosomal protein L1	Ribosome	25.9	238	2.6E + 07	1.7E + 07	1.5E + 08	1.8E + 08	3.5E + 08	2.2E + 08
Slr2051 PBS rod core linker CpcG1	PS antenna	28.9	249	2.4E + 08	6.5E + 07	9.3E + 07	1.7E + 08	1.1E + 07	7.5E + 07
Sll1579 PBS rod linker CpcC2	PS antenna	30.8	273	2.6E + 08	5.7E + 07	4.6E + 07	1.3E + 08	1.6E + 07	5.6E + 07
Slr2018 unknown protein	None	84.9	799	1.6E + 08	8.3E + 07	2.1E + 08	1.2E + 07	1.0E + 08	0
Slr1986 ApcB	PS antenna	17.2	161	1.6E + 08	0	3.9E + 07	1.1E + 08	2.3E + 07	9.6E + 07

The experiment was performed in biological triplicates, indicated by the numbers 1 to 3. The protein abundance is color-coded from red (low) to green (high). MW, molecular weight in kDa; PBS, phycobilisome; n/a, not applicable.

blot approach (66). In this assay, the attached 6×His tag was then recognized by an antiserum coupled to horseradish–peroxidase, providing a signal for proteins bound to the fusion protein (Fig. 5*A*). The signal in the blot overlapped with the CpcB band at ∼18 kDa, one of the most prominent proteins visible by sodium dodecyl sulfate polyacrylamide gel electrophoresis (SDS-PAGE) (Fig. 5*B*). We included controls to exclude nonspecific cross reaction of the fusion protein: a *Synechocystis* 6803 mutant lacking genes for CpcA and CpcB [Δ*cpc* (67)], and an *Escherichia coli* lysate. Furthermore, recombinant apo-CpcB with a Strep tag was also investigated in this regard (Fig. 5*C*). We did not detect any signal in these controls, underlining the specificity of NblD-binding to CpcB. To investigate whether NblD would also bind to the apo–CpcB form, recombinant CpcB was produced in *E. coli*. Again, the far western signal was obtained for the lysate from *Synechocystis* 6803 but not the Δ*cpc* strain. The antiserum directed against the His tag detected also the His-tagged CpcB produced in *E. coli*; furthermore, production of recombinant CpcB was verified by detection of a Strep-tagged variant (Fig. 5*C*). Thus, apo-CpcB lacking chromophores or possible cyanobacteria-specific posttranslational modifications was not sufficient to enable the binding of NblD. These results suggest that NblD specifically interacts with chromophorylated CpcB; however, both subunits of PC were enriched in the coimmunoprecipitation due to the strong natural heterodimer formation between them.

Incubation of phycobilisomes isolated from *Synechocystis* 6803 wild-type and Δ*nblD* with recombinant NblD in vitro led to a reduction in fluorescence as opposed to phycobilisomes without added protein or with added SUMO protein (Fig. 5*D* and *SI Appendix*, Figs. S5 and S6). It made no difference whether the phycobilisomes were prepared from nitrogen-replete or -deplete cultures (Fig. 5*D*). Moreover, the ratio of PC and APC peaks differed dramatically between control samples, and phycobilisomes treated with NblD and a 640-nm "shoulder" appeared. For comparison, we added urea at concentrations aiding the dissociation of phycobilisome complexes (68), leading to reduced signal intensities and loss of the APC signal in both excitation and emission spectra at 650 nm and 680 nm, respectively. Next, we followed the NblD effect on isolated phycobilisomes in a time course experiment (*SI Appendix*, Fig. S5). Room temperature absorbance spectroscopy showed a broadening and shift of the peak at 625 nm to lower wavelengths. A similar effect was observed when different concentrations of urea were added (*SI Appendix*, Fig. S5*C*).

The Presence of *nblD* Is Positively Selected in Competition Experiments. We speculated that the lack of NblD might also have a growth effect. However, in short-term growth experiments, *nblD* deletion strains showed no noticeable growth effect (*SI Appendix*, Fig. S3) despite the strong nonbleaching phenotype under nitrogen-starvation conditions (Fig. 3). Therefore, we set up a growth competition experiment for a longer period in medium containing only 1 mM $NaNO_3$ as the sole source of nitrogen. In this setting, the Δ*nblD* mutant was out-competed by the wild-type after 12 generations (*SI Appendix*, Fig. S7). These findings directly support the physiological importance of NblD, while its evolutionary conservation suggests that the presence of NblD has been under positive selection in cyanobacteria.

Discussion

The acclimation of cyanobacteria to nitrogen starvation is a complex physiological process governed by a particular genetic program (10) and involves many proteins and regulatory RNAs with different roles. The main goal of this finely tuned process is a reversible dormant state that is entered until a new source of nitrogen appears. Although cyanobacteria can produce excess phycobiliproteins (69) that can be degraded as a source of reduced nitrogen without affecting photosynthesis or growth rate, many species use a particular strategy to cope with periods of nitrogen starvation, known as chlorosis (18, 19). Hence, antenna complexes are diminished, and light harvesting becomes reduced. The results of in vitro experiments with *Synechocystis*

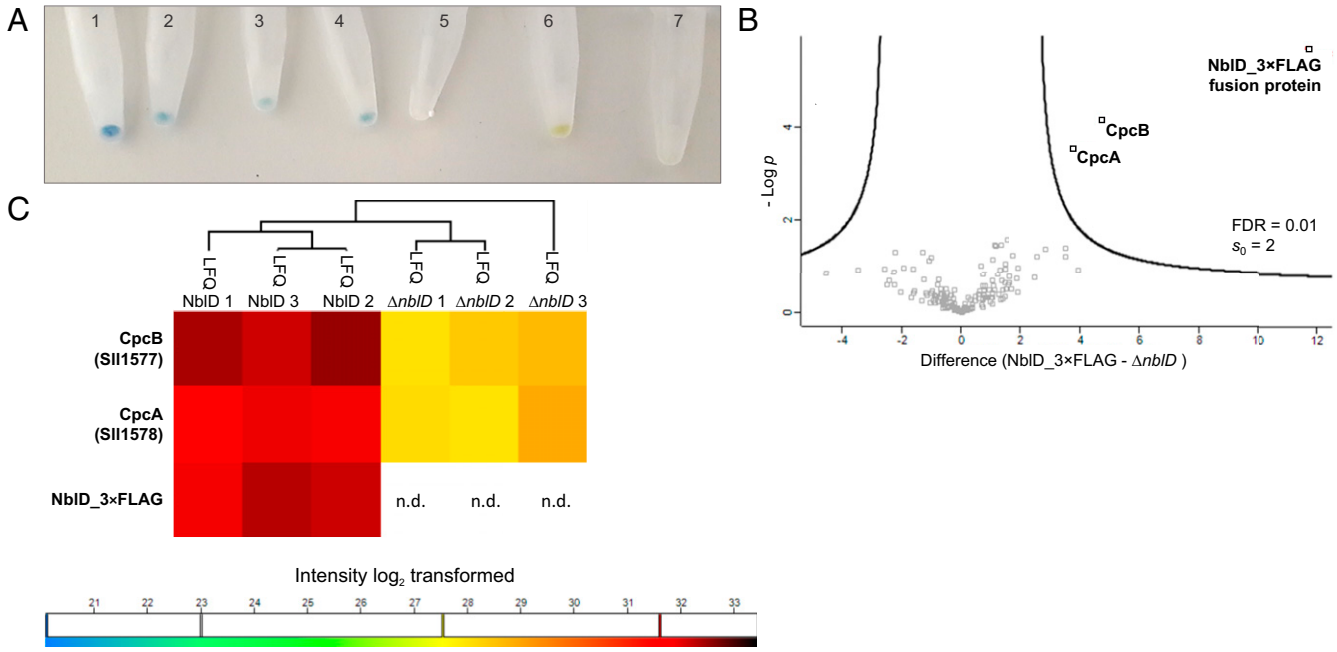

Fig. 4. Enrichment of phycobilisome proteins in NblD pull-down experiments from cultures 3 h after nitrogen removal. (*A*) The collected samples with FLAG-tagged proteins in affinity gels after the final wash step and before the elution were initially incubated as follows: 1 to 4: lysates containing nblD_3×FLAG; 5: incubated with Δ*nblD* lysate; 6: lysate containing norf1_3×FLAG (50); 7: lysate containing sfGFP_3×FLAG. (*B*) Volcano plot based on a two-sample *t* test of enriched proteins using a false discovery rate (FDR) of 0.01 and a coefficient for variance minimization (85) s_0 of 2. (*C*) Hierarchical clustering of the most abundant proteins detected in the MS indicating higher $\log_2$-transformed LFQ intensities for the PC subunits in the NblD_3×FLAG–containing samples. NblD was not detected (n.d.) in the knockout samples of Δ*nblD*. Numerical details of the data analyses in *B* and *C* are given in the *SI Appendix*, Tables S4 and S5. The pull-down experiment was repeated twice at the same facility and a third time at another proteomics facility and 24 h after nitrogen removal (*SI Appendix*, Fig. S9), and comparable results were obtained.

6803 lyases, biliproteins, and NblA/B implied complex interactions between these factors and processes during phycobilisome degradation (68). NblD, a small protein, is strongly up-regulated under nitrogen starvation in *Synechocystis* 6803 (50) and, as shown in this study, participates in phycobilisome disassembly. Other Nbl proteins involved in the disintegration of phycobilisome antenna complexes have been characterized in different cyanobacteria in detail, but most insight has been obtained in *S. elongatus* 7942. The expression of *nblA* genes is strongly induced in both species under nitrogen starvation. NblA was found to interact with the PC rod antenna structure at a specific groove in CpcB (31) but also targeting the APC core (70), while NblB was characterized as a chromophore-detaching protein affecting PC and APC (71). The likely ortholog of the *S. elongatus nblB* gene in *Synechocystis* 6803 is *nblB1*, whose expression was decreased under nitrogen starvation (*SI Appendix*, Table S1) like the *S. elongatus* gene (71). It is noteworthy that knockout mutants of homologs to five *S. elongatus nbl* genes were tested in *Synechocystis* 6803, but only Δ*nblA1* and Δ*nblA2* displayed the nonbleaching phenomenon (33). Later on, Δ*sll1961* lacking the GntR-family transcriptional regulator Sll1961 was discovered to also yield this phenotype (72). Hence, Δ*nblD* is the fourth mutant with the *nbl* phenotype in *Synechocystis* 6803. Considering the function of NblD, we first investigated the possibility that NblD could act as a regulator or coregulator of gene expression. However, except a slight increase in *nblB2* mRNA accumulation, no pronounced effect on the expression of *nbl* genes was found in Δ*nblD*. We detected an increased transcript level for three of four *hli* genes and the *hliB/scpD* cotranscribed *lilA* (*slr1544*) gene in Δ*nblD* (*SI Appendix*, Table S1 and Fig. S2). These genes encode small proteins with an anticipated function in transiently storing chlorophyll molecules during situations causing stress for the photosynthetic apparatus (73–75). Furthermore, the transcript levels of a few other genes encoding proteins participating in stress responses, like *pgr5* (*ssr2016*) and *sigD* (*sll2012*), were slightly increased in the mutant (*SI Appendix*, Table S1 and Fig. S2) but the results were far from showing relevant dysregulation of gene expression. Hence, NblD is not a transcriptional regulator or coregulator.

In our coimmunoprecipitation and far Western blot analyses, we observed the interaction of NblD with CpcB, which is a striking parallel to NblA, the main factor for phycobilisome degradation by recruitment of a Clp-like protease (32, 76). However, we can also rule out a function of NblD as protease adaptor because no protease subunits were found in our interaction screens, and its ectopic overexpression under nutrient-replete conditions did not trigger bleaching (Fig. 3*A*). We also did not find an interaction with NblA or a likely direct regulatory effect excluding roles as coeffector of NblA. The only detected interaction was with chromophorylated CpcB. Phycocyanobilin chromophores are covalently bound at CpcB cysteine residues 84 and 155 and are visible by zinc-induced fluorescence even during SDS-PAGE and in protein pull-down experiments (Fig. 4*A*). These features enabled the far Western blot signal for tagged NblD as bait protein bound to the chromophorylated target on the membrane but not to the recombinant apo-CpcB (Fig. 5*C*). The chromophores likely also remained covalently bound to their binding partner CpcB during the affinity-based enrichment preceding MS. Moreover, we found that in the absence of NblD, the chromophorylated target remained highly abundant under nitrogen depletion. These findings point at a pivotal role of NblD as a possible cofactor in opening the tight phycobilisome structure, eventually leading to the disruption of PC hexamers and making them accessible for NblA/Clp action. Recent studies suggested that the large NblA/ClpC complex involved in phycobilisome degradation does not fit into the predicted interaction groove (31).

According to our data, NblD is involved in the genetic program governing the acclimation response to nitrogen starvation (Fig. 6). We propose a hierarchically organized process of

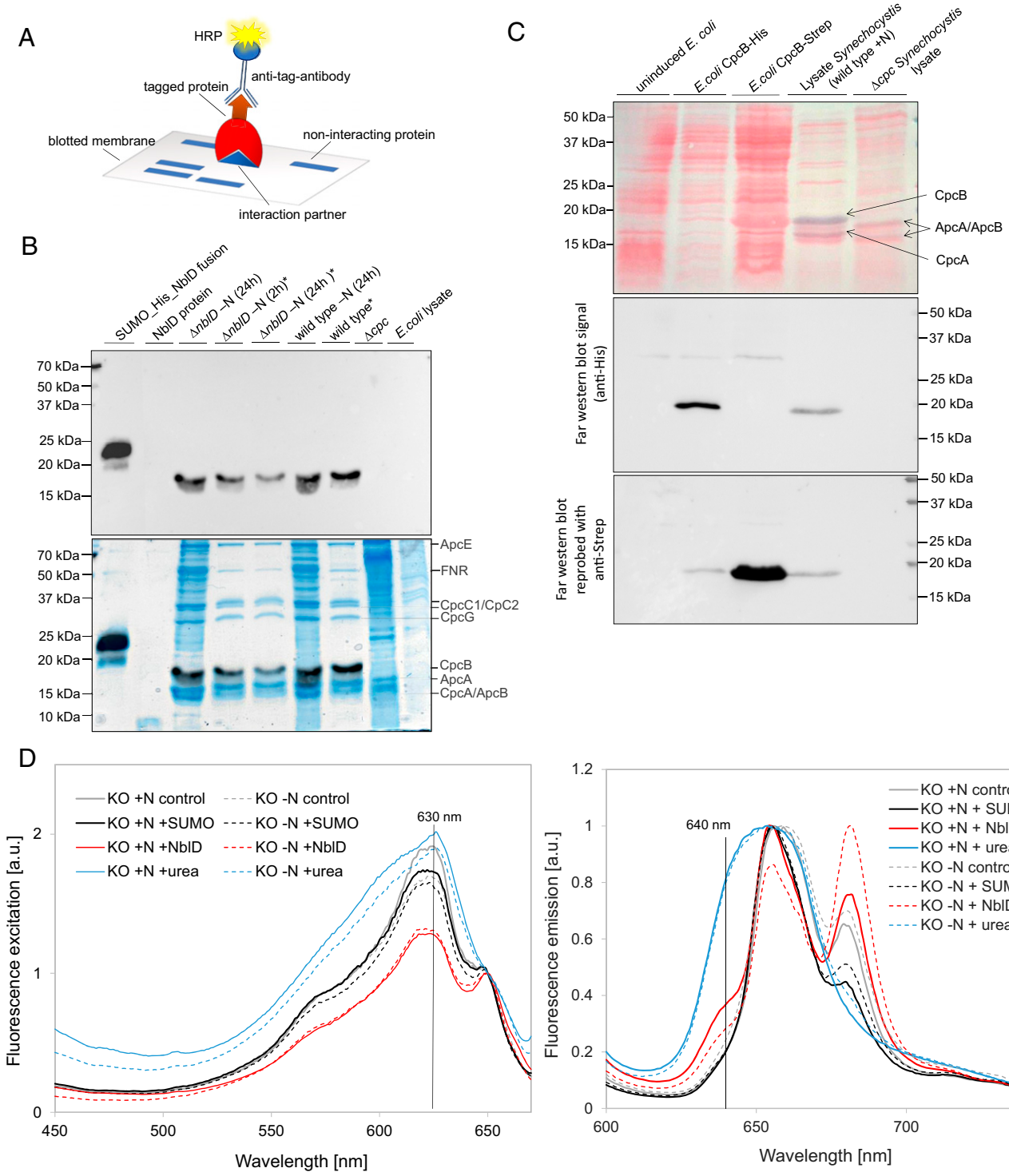

Fig. 5. Far Western blot analysis. (*A*) General principle for the detection of protein–protein interactions by far Western blotting using a tagged protein to probe potential interaction partners blotted on a membrane. An antiserum, coupled to horseradish peroxidase (HRP), targets the protein tag, here a 6×His-tag. (*B*) Far Western blot signal probing the interactions of the His-tagged NblD-fusion protein (*Upper*). The immunoblot signal was merged with the stained gel image (*Lower*) to visualize that the signal overlaps with the stained CpcB subunit. Purified phycobilisome samples are marked with asterisks and the respective proteins are annotated on the right. (*C*, *Upper*) Ponceau S-stained membrane. The highly abundant phycobiliproteins show a characteristic blueish signal and are marked with arrows, CpcA and CpcB are lacking in the Δ*cpc* mutant (67). (*Middle*) Far Western blot signal using His-tagged NblD-fusion protein. (*Lower*) Strep-tag–based verification of apo–CpcB expression. (*D*) Low-temperature excitation spectra (*Left*) and emission spectra (*Right*) at 77 K for 100 μg phycobilisomes (PBS) isolated from the Δ*nblD* (KO) mutant cultivated with (solid lines) and without nitrogen for 3 h (dashed lines). Phycobilisome preparations were incubated with either SUMO–NblD fusion protein (red), SUMO protein (black), or urea (3 M final concentration, blue). As a control, proteins and urea were omitted (gray). Low-temperature excitation spectra were recorded five times, averaged, and normalized to the APC maximum at 650 nm. Low-temperature emission spectra at 580-nm excitation were recorded three times, averaged, and normalized to their respective maximum peaks.

phycobilisome degradation, with NblD starting above NblA in *Synechocystis* 6803. Consequently, if any component is missing in the chain of the nitrogen starvation–triggered disassembly process, a nonbleaching phenotype is obtained. We show that NblD contains four cysteines arranged in two clusters and that a change in the first pair of cysteines results in an appearance similar to the knock-out (Fig. 3 *A* and *B*). Thus, an important function of these conserved aa can be assumed.

The observed specificity of NblD in binding only to chromophorylated CpcB in the far Western blot analysis suggests that phycocyanobilin is required for the interaction with CpcB, either directly or indirectly. NblD alone did not trigger phycobilisome decomposition as shown in the in vitro assay (*SI Appendix*, Fig. S6), as other factors, like NblA and NblB, needed for further degradation steps might not cosediment with the phycobilisome fraction during purification.

We show that NblD is a factor in the process that leads to the coordinated dismantling of phycobilisomes. Similar to the NblA proteins that label phycobiliproteins for proteolysis, NblD binds to PC polypeptides but has a different function. The results show that, even in a well-studied process such as the bleaching response, small proteins can perform crucial functions that have been overlooked thus far.

Materials and Methods

Cultivation Conditions. Strains were maintained in copper-free BG11 (52) supplemented with 20 mM TES (Roth) pH 7.5 under continuous white light of 50 μmol photons $m^{-2} \cdot s^{-1}$ at 30 °C. Mutant strains containing pVZ322 were cultivated in the presence of 50 μg/mL kanamycin and 25 μg/mL gentamycin, while Δ*nblD* was kept at 50 μg/mL kanamycin. For nitrogen depletion, the cultures were centrifuged (8 min, 3,200 × *g*) and the cell pellets washed and resuspended in BG11 without $NaNO_3$ (BG11-N). Cultures in phenotypic assays were grown in medium supplemented with copper-lacking antibiotics to prevent any possible side effect.

Construction of Mutant and Overexpression Lines. *Synechocystis* 6803 PCC-M (77) was used as the wild-type and background for the construction of mutants. Knockout mutants were generated by homologous replacement of the *nblD* coding sequence with a kanamycin resistance cassette (*nptII*) and using pUC19 as a vector for subcloning. The construct for gene replacement was generated by Advanced Quick Assembly (AQUA) cloning (78). Details of primer sequences and plasmids are given in *SI Appendix*, Tables S2 and S3. Segregation of *nblD* and Δ*nblD*/*nptII* alleles was checked by colony PCR using the primers segregation_nblD_KO fwd/rev and nblD_Km_seq fwd/rev (*SI Appendix*, Fig. S1).

To complement the knockout and study NblD functions further, different versions of *nblD* were inserted into the self-replicating pVZ322 plasmid (primers and vectors are listed in *SI Appendix*, Tables S1 and S2): 1) providing *nblD* under control of its native promotor (50) to restore wild type; 2) expressing *nblD* under control of the Cu^{2+}-inducible *petE* promoter (50); 3) same plasmid as in "1" but encoding a cysteine-mutated version of NblD (C9S and C12S); and 4) same plasmid as in "1" but with a premature stop codon (Ser2"STOP").

The inserts for pVZ322 were assembled into pUC19 by AQUA cloning and then digested, as well as the target pVZ322 vector backbone, for 3.5 h at 37 °C by *Xba*I and *Pst*I, producing compatible ligation sites. Fragments were ligated with T4 DNA ligase (Thermo Fisher Scientific) for 4 h at room temperature and propagated in *E. coli*. The sequence-verified plasmids were introduced into *Synechocystis* 6803 by conjugation (79). The expression levels of *nblD* in the different lines was checked by northern hybridization using a ^{32}P-labeled, single-stranded RNA probe produced using the primer T7_nsiR6_probe fwd/rev.

Protein Preparation, Proteomic Sample Preparation, and Analyses by MS. Cells to prepare total protein samples were collected by centrifugation (3,200 × *g*, 10 min, at room temperature [RT]), washed in phosphate-buffered saline supplemented with Protease Inhibitor (cOmplete, Roche) and resuspended in the same buffer. For cell lysis, mechanical disruption using a prechilled Precellys homogenizer (Bertin Technologies) was used. To remove cell debris and glass beads, the culture was centrifuged (1,000 × *g*, 5 min, 4 °C), and the supernatant was collected for further analysis. Western blots targeting FLAG-tagged proteins were performed using FLAG M2 monoclonal antibody (Sigma) as described previously (50).

To prepare FLAG-tagged NblD and interacting proteins from total-cell lysates and to process mock samples, ANTI-FLAG M2 affinity agarose gel matrix (Sigma) was used. The expression of *nblD* was induced in exponentially growing cultures (800 mL at optical density [OD] 0.8) by removing nitrogen. After another 3 h of cultivation, the cells were harvested by centrifugation (4,000 × *g*, 4 °C, 10 min). Cell lysates were obtained as described above (except using FLAG buffer instead of phosphate buffered saline) and then were incubated for 45 min in the presence of 2% n-dodecyl β-D-maltoside to solubilize membrane proteins in the dark at 4 °C. After loading the lysate into the packed volume of 100 μL of FLAG agarose on a gravity column (Bio-Rad) and reloading the flow through twice, bound proteins were washed three times with FLAG buffer (50 mM Hepes-NaOH pH 7, 5 mM $MgCl_2$, 25 mM $CaCl_2$, 150 mM NaCl, 10% glycerol, 0.1% Tween-20) and twice with FLAG buffer lacking glycerol and Tween-20.

To achieve maximum reproducibility, protein analyses by MS were performed in two different laboratories and repeated several times. To obtain MS data, elution was performed using 0.2% RapiGest (Waters) in 0.1 M Hepes pH 8 (MS-grade) and heating for 10 min to 95 °C. The RapiGest concentration was decreased to 0.1% by adding 0.1 M Hepes pH 8. The proteins were reduced by incubating in 5 mM DTT and alkylated using 15 mM iodoacetamide in the dark, with each step performed for 20 min at 37 °C. Tryptic digestion was performed in two steps: first with 1 μg trypsin for 2 h at 50 °C and second with another 1 μg overnight at 37 °C, both shaking at 600 rpm. The peptides were desalted by acidification of the sample to 0.3% trifluoroacetic acid final concentration and applying HyperSep C18 tips (Thermo Fisher Scientific). Thereafter, the peptide concentration was measured using the bicinchoninic acid assay (Thermo Fisher Scientific). For MS analysis, 500 ng of peptide per sample was analyzed using the EASY-nLC

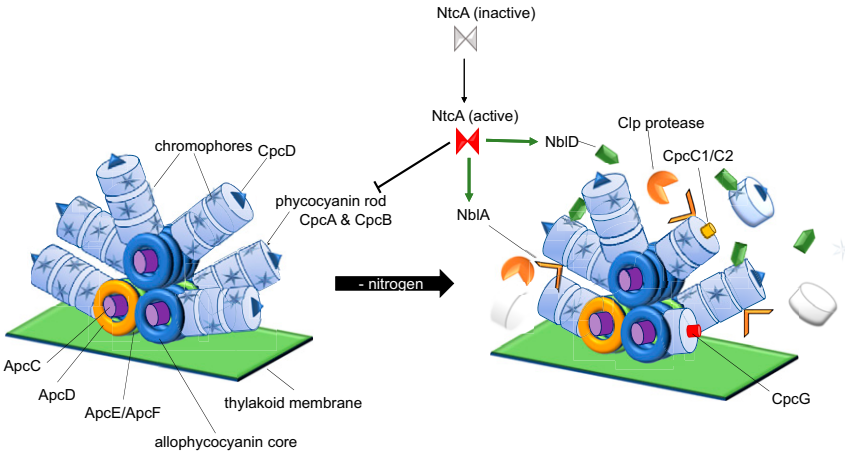

Fig. 6. Proposed model for the integration of NblD into the genetic program to respond to nitrogen starvation and its role in phycobilisome degradation in the early phase of nitrogen depletion. The *Synechocystis* phycobilisome consists of six PC rods, each composed of three PC hexamers, that extend from the core formed by three APC core cylinders (86). The position of the trimers containing ApcD or ApcE/ApcF is indicated. The positions of ApcC, CpcD, CpC1/2, and CpcG are also given. Chromophores are delineated as stars. NtcA, the major transcriptional regulator of the response to low nitrogen, activates transcription of the *nblD* and *nblA* genes (green arrows) while it represses the transcription of the *cpcBAC2C1D* operon (17) encoding the PC rod and linker proteins. NblA targets CpcB as protease adaptor recruiting Clp protease. Our data show that NblD interacts with CpcB as well but has another function, likely in opening the tight phycobilisome structure to disrupt PC hexamers, freeing them up for tagging and degradation by the NblA–Clp system and removal of the bilin chromophores by enzymes involved in this process such as NblB (68, 71).

1000 UHPLC system (Thermo Fisher Scientific) coupled to a Q-Exactive plus Hybrid Quadrupole-Orbitrap Mass Spectrometer (Thermo Fisher Scientific) as previously described (80). Raw data were processed and analyzed with MaxQuant (Version 1.6.0.16) using cyanobase (81) data for *Synechocystis* 6803 (Version 2018/08/01) including the small proteins described in reference (50). The proteome raw data acquired by MS were deposited at the ProteomeXchange Consortium (proteomecentral.proteomexchange.org) via the PRIDE partner repository (82) under the identifier PXD019019. The intensities were compared using LFQ (label-free quantification) values (83) as illustrated in *SI Appendix*, Fig. S8 with Perseus [version 1.6.1.3 (84)]. In summary, contaminants, reverse sequences, and proteins only identified by site were removed from the matrix, and LFQ intensities were $\log_2$-transformed. Before *t* test and visualization using a volcano plot, the missing values were replaced by imputation with the normal distribution for each column separately (default settings). For hierarchical clustering (default parameters), only proteins with three valid values in at least one declared group (NblD_3×FLAG and Δ*nblD*) were considered.

Far Western Blotting. Far Western blotting was performed as described previously (66) using purified NblD-SUMO-His–tag fusion protein instead of the primary antibody in the original Western blot procedure. In the denaturing/renaturing steps of the blotted membrane, milk powder was omitted compared with the protocol provided by Wu et al. (66). Between steps, the membrane was washed with Tris(hydroxymethyl)aminomethan buffered saline plus Tween (TBS-T; 20 mM Tris pH 7.6, 150 mM NaCl, 0.1% [vol/vol] Tween-20). After blocking the renatured membrane with 5% milk powder in TBS-T, 3 μg/mL of fusion protein was used for the primary interaction and incubated at 4 °C for at least 6 h. His-Penta-Conjugate (Qiagen) was then used as antiserum (1:5,000), targeting the 6×His-tag of the NblD-fusion protein, with shaking at 4 °C for a minimum of 6 h. The membranes were washed in between the single steps at least twice with TBS-T for 5 min at RT. The signals were visualized by applying ECL-spray (Advansta) to the membrane and using a Fusion FX (Vilber) imager.

Additional detailed materials and methods are provided in *SI Appendix, Supplementary Methods*. This includes information on RNA preparation, microarray analysis and Northern blot verification, recombinant protein expression and purification, spectrometric measurements, phycobilisome isolation, measuring NblD activity in vitro, SDS-PAGE and Western blotting, and competition growth assays.

Data Availability. Study data are included in the article and *SI Appendix*. Gene expression data and proteomics data have been deposited in Gene Expression Omnibus and PRIDE partner repository (GSE149511 and PXD019019).

ACKNOWLEDGMENTS. We are very grateful to Tasios Melis (University of California, Berkeley, CA), who kindly provided the PC mutant for the far Western blot analysis. We also thank Martin Hagemann (Rostock), Heiko Lokstein (Prague), Jörg Soppa and Harald Schwalbe (both Frankfurt), and Mai Watanabe and Annegret Wilde (both Freiburg) for helpful discussions and Annegret Wilde for access to the spectrophotometer. Furthermore, we thank Viktoria Reimann for helping with the microarray and Stefan Tuskan for support in setting up the competition assay experiment. We appreciate the support by the Deutsche Forschungsgemeinschaft (DFG, German Research Foundation) to W.R.H. through the priority program "Small Proteins in Prokaryotes, an Unexplored World" SPP 2002 (grant DFG HE2544/12-1); to P.S., B.M., and W.R.H. through the research group FOR2816 "SCyCode"; and to V.K., O.S., and W.R.H. through the graduate school MeInBio (322977937/GRK2344). O.S. acknowledges support by DFG (SCHI 871/11-1).

1. M. M. M. Kuypers, H. K. Marchant, B. Kartal, The microbial nitrogen-cycling network. *Nat. Rev. Microbiol.* **16**, 263–276 (2018).
2. P. M. Vitousek, R. W. Howarth, Nitrogen limitation on land and in the sea: How can it occur? *Biogeochemistry* **13**, 87–115 (1991).
3. S. J. Biller, P. M. Berube, D. Lindell, S. W. Chisholm, *Prochlorococcus*: The structure and function of collective diversity. *Nat. Rev. Microbiol.* **13**, 13–27 (2015).
4. P. Flombaum *et al*., Present and future global distributions of the marine Cyanobacteria *Prochlorococcus* and *Synechococcus*. *Proc. Natl. Acad. Sci. U.S.A.* **110**, 9824–9829 (2013).
5. F. Partensky, W. R. Hess, D. Vaulot, *Prochlorococcus*, a marine photosynthetic prokaryote of global significance. *Microbiol. Mol. Biol. Rev.* **63**, 106–127 (1999).
6. M. Hagemann, W. R. Hess, Systems and synthetic biology for the biotechnological application of cyanobacteria. *Curr. Opin. Biotechnol.* **49**, 94–99 (2018).
7. D. Vijay, M. K. Akhtar, W. R. Hess, Genetic and metabolic advances in the engineering of cyanobacteria. *Curr. Opin. Biotechnol.* **59**, 150–156 (2019).
8. R. Schwarz, K. Forchhammer, Acclimation of unicellular cyanobacteria to macronutrient deficiency: Emergence of a complex network of cellular responses. *Microbiology (Reading)* **151**, 2503–2514 (2005).
9. K. Forchhammer, R. Schwarz, Nitrogen chlorosis in unicellular cyanobacteria - a developmental program for surviving nitrogen deprivation. *Environ. Microbiol.* **21**, 1173–1184 (2019).
10. A. Klotz *et al*., Awakening of a dormant cyanobacterium from nitrogen chlorosis reveals a genetically determined program. *Curr. Biol.* **26**, 2862–2872 (2016).
11. M. F. Vázquez-Bermúdez, A. Herrero, E. Flores, 2-Oxoglutarate increases the binding affinity of the NtcA (nitrogen control) transcription factor for the *Synechococcus glnA* promoter. *FEBS Lett.* **512**, 71–74 (2002).
12. R. Tanigawa *et al*., Transcriptional activation of NtcA-dependent promoters of *Synechococcus* sp. PCC 7942 by 2-oxoglutarate in vitro. *Proc. Natl. Acad. Sci. U.S.A.* **99**, 4251–4255 (2002).
13. J. Espinosa, K. Forchhammer, S. Burillo, A. Contreras, Interaction network in cyanobacterial nitrogen regulation: PipX, a protein that interacts in a 2-oxoglutarate dependent manner with PII and NtcA. *Mol. Microbiol.* **61**, 457–469 (2006).
14. J. Espinosa *et al*., PipX, the coactivator of NtcA, is a global regulator in cyanobacteria. *Proc. Natl. Acad. Sci. U.S.A.* **111**, E2423–E2430 (2014).
15. A. Forcada-Nadal, J. L. Llácer, A. Contreras, C. Marco-Marín, V. Rubio, The PII-NAGK-PipX-NtcA regulatory axis of cyanobacteria: A tale of changing partners, allosteric effectors and non-covalent interactions. *Front. Mol. Biosci.* **5**, 91 (2018).
16. M. I. Muro-Pastor, J. C. Reyes, F. J. Florencio, Cyanobacteria perceive nitrogen status by sensing intracellular 2-oxoglutarate levels. *J. Biol. Chem.* **276**, 38320–38328 (2001).
17. J. Giner-Lamia *et al*., Identification of the direct regulon of NtcA during early acclimation to nitrogen starvation in the cyanobacterium *Synechocystis* sp. PCC 6803. *Nucleic Acids Res.* **45**, 11800–11820 (2017).
18. M. M. Allen, A. J. Smith, Nitrogen chlorosis in blue-green algae. *Arch. Mikrobiol.* **69**, 114–120 (1969).
19. M. Görl, J. Sauer, T. Baier, K. Forchhammer, Nitrogen-starvation-induced chlorosis in *Synechococcus* PCC 7942: Adaptation to long-term survival. *Microbiology (Reading)* **144**, 2449–2458 (1998).
20. N. Adir, S. Bar-Zvi, D. Harris, The amazing phycobilisome. *Biochim. Biophys. Acta Bioenerg.* **1861**, 148047 (2020).
21. A. N. Glazer, "Phycobilisomes" in *Cyanobacteria*, L. Packer, A. N. Glazer, Eds. (Methods in Enzymology, Elsevier, 1988), vol. 167, pp. 304–312.
22. R. MacColl, Cyanobacterial phycobilisomes. *J. Struct. Biol.* **124**, 311–334 (1998).
23. A. R. Grossman, M. R. Schaefer, G. G. Chiang, J. L. Collier, The phycobilisome, a light-harvesting complex responsive to environmental conditions. *Microbiol. Rev.* **57**, 725–749 (1993).
24. J. L. Collier, A. R. Grossman, Chlorosis induced by nutrient deprivation in *Synechococcus* sp. strain PCC 7942: Not all bleaching is the same. *J. Bacteriol.* **174**, 4718–4726 (1992).
25. P. Spät, A. Klotz, S. Rexroth, B. Maček, K. Forchhammer, Chlorosis as a developmental program in cyanobacteria: The proteomic fundament for survival and awakening. *Mol. Cell. Proteomics* **17**, 1650–1669 (2018).
26. J. L. Collier, A. R. Grossman, A small polypeptide triggers complete degradation of light-harvesting phycobiliproteins in nutrient-deprived cyanobacteria. *EMBO J.* **13**, 1039–1047 (1994).
27. R. Schwarz, A. R. Grossman, A response regulator of cyanobacteria integrates diverse environmental signals and is critical for survival under extreme conditions. *Proc. Natl. Acad. Sci. U.S.A.* **95**, 11008–11013 (1998).
28. K. Baier, S. Nicklisch, C. Grundner, J. Reinecke, W. Lockau, Expression of two *nblA*-homologous genes is required for phycobilisome degradation in nitrogen-starved *Synechocystis* sp. PCC6803. *FEMS Microbiol. Lett.* **195**, 35–39 (2001).
29. I. Luque *et al*., The NblAI protein from the filamentous cyanobacterium Tolypothrix PCC 7601: Regulation of its expression and interactions with phycobilisome components. *Mol. Microbiol.* **50**, 1043–1054 (2003).
30. R. Bienert, K. Baier, R. Volkmer, W. Lockau, U. Heinemann, Crystal structure of NblA from *Anabaena* sp. PCC 7120, a small protein playing a key role in phycobilisome degradation. *J. Biol. Chem.* **281**, 5216–5223 (2006).
31. A. Y. Nguyen *et al*., The proteolysis adaptor, NblA, binds to the N-terminus of β-phycocyanin: Implications for the mechanism of phycobilisome degradation. *Photosynth. Res.* **132**, 95–106 (2017).
32. A. Karradt, J. Sobanski, J. Mattow, W. Lockau, K. Baier, NblA, a key protein of phycobilisome degradation, interacts with ClpC, a HSP100 chaperone partner of a cyanobacterial Clp protease. *J. Biol. Chem.* **283**, 32394–32403 (2008).
33. H. Li, L. A. Sherman, Characterization of Synechocystis sp. strain PCC 6803 and deltanbl mutants under nitrogen-deficient conditions. *Arch. Microbiol.* **178**, 256–266 (2002).
34. G. Zabulon, C. Richaud, C. Guidi-Rontani, J.-C. Thomas, NblA gene expression in Synechocystis PCC 6803 strains lacking DspA (Hik33) and a NblR-like protein. *Curr. Microbiol.* **54**, 36–41 (2007).
35. M. Lluch-Senar *et al*., Defining a minimal cell: Essentiality of small ORFs and ncRNAs in a genome-reduced bacterium. *Mol. Syst. Biol.* **11**, 780 (2015).
36. S. Meydan *et al*., Retapamulin-Assisted ribosome profiling reveals the alternative bacterial proteome. *Mol. Cell* **74**, 481–493.e6 (2019).
37. J. Weaver, F. Mohammad, A. R. Buskirk, G. Storz, Identifying small proteins by ribosome profiling with stalled initiation complexes. *mBio* **10**, e02819-18 (2019).
38. A. Guskov *et al*., Cyanobacterial photosystem II at 2.9-A resolution and the role of quinones, lipids, channels and chloride. *Nat. Struct. Mol. Biol.* **16**, 334–342 (2009).
39. Y. Kashino *et al*., Proteomic analysis of a highly active photosystem II preparation from the cyanobacterium *Synechocystis* sp. PCC 6803 reveals the presence of novel polypeptides. *Biochemistry* **41**, 8004–8012 (2002).
40. P. Fromme, A. Melkozernov, P. Jordan, N. Krauss, Structure and function of photosystem I: Interaction with its soluble electron carriers and external antenna systems. *FEBS Lett.* **555**, 40–44 (2003).

41. D. Baniulis *et al*., Structure-function, stability, and chemical modification of the cyanobacterial cytochrome b6f complex from *Nostoc* sp. PCC 7120. *J. Biol. Chem.* **284**, 9861–9869 (2009).
42. J. F. Allen, Cytochrome b6f: Structure for signalling and vectorial metabolism. *Trends Plant Sci.* **9**, 130–137 (2004).
43. D. Schneider, T. Volkmer, M. Rögner, G. Pet, N. Pet, PetG and PetN, but not PetL, are essential subunits of the cytochrome b6f complex from Synechocystis PCC 6803. *Res. Microbiol.* **158**, 45–50 (2007).
44. M. M. Nowaczyk *et al*., NdhP and NdhQ: Two novel small subunits of the cyanobacterial NDH-1 complex. *Biochemistry* **50**, 1121–1124 (2011).
45. J. Knoppová *et al*., Discovery of a chlorophyll binding protein complex involved in the early steps of photosystem II assembly in *Synechocystis*. *Plant Cell* **26**, 1200–1212 (2014).
46. E. C. Hobbs, F. Fontaine, X. Yin, G. Storz, An expanding universe of small proteins. *Curr. Opin. Microbiol.* **14**, 167–173 (2011).
47. M. Kopf *et al*., Comparative analysis of the primary transcriptome of *Synechocystis* sp. PCC 6803. *DNA Res.* **21**, 527–539 (2014).
48. M. Kopf, S. Klähn, I. Scholz, W. R. Hess, B. Voß, Variations in the non-coding transcriptome as a driver of inter-strain divergence and physiological adaptation in bacteria. *Sci. Rep.* **5**, 9560 (2015).
49. J. Mitschke *et al*., An experimentally anchored map of transcriptional start sites in the model cyanobacterium *Synechocystis* sp. PCC6803. *Proc. Natl. Acad. Sci. U.S.A.* **108**, 2124–2129 (2011).
50. D. Baumgartner, M. Kopf, S. Klähn, C. Steglich, W. R. Hess, Small proteins in cyanobacteria provide a paradigm for the functional analysis of the bacterial micro-proteome. *BMC Microbiol.* **16**, 285 (2016).
51. A. Kamei, T. Yuasa, K. Orikawa, X. X. Geng, M. Ikeuchi, A eukaryotic-type protein kinase, SpkA, is required for normal motility of the unicellular Cyanobacterium *synechocystis* sp. strain PCC 6803. *J. Bacteriol.* **183**, 1505–1510 (2001).
52. R. Rippka, J. Deruelles, J. B. Waterbury, M. Herdman, R. Y. Stanier, Generic assignments, strain histories and properties of pure cultures of cyanobacteria. *Microbiology* **111**, 1–61 (1979).
53. D. Lhee *et al*., Evolutionary dynamics of the chromatophore genome in three photosynthetic *Paulinella* species. *Sci. Rep.* **9**, 2560 (2019).
54. E. C. M. Nowack, M. Melkonian, G. Glöckner, Chromatophore genome sequence of Paulinella sheds light on acquisition of photosynthesis by eukaryotes. *Curr. Biol.* **18**, 410–418 (2008).
55. D. Bombar, P. Heller, P. Sanchez-Baracaldo, B. J. Carter, J. P. Zehr, Comparative genomics reveals surprising divergence of two closely related strains of uncultivated UCYN-A cyanobacteria. *ISME J.* **8**, 2530–2542 (2014).
56. J. P. Zehr *et al*., Globally distributed uncultivated oceanic N2-fixing cyanobacteria lack oxygenic photosystem II. *Science* **322**, 1110–1112 (2008).
57. F. Partensky *et al*., A novel species of the marine cyanobacterium *Acaryochloris* with a unique pigment content and lifestyle. *Sci. Rep.* **8**, 9142 (2018).
58. S. S. Krishna, I. Majumdar, N. V. Grishin, Structural classification of zinc fingers: Survey and summary. *Nucleic Acids Res.* **31**, 532–550 (2003).
59. V. Y. Tarasov *et al*., A small protein from the *bop-brp* intergenic region of *Halobacterium salinarum* contains a zinc finger motif and regulates *bop* and *crtB1* transcription. *Mol. Microbiol.* **67**, 772–780 (2008).
60. A. Waterhouse *et al*., SWISS-MODEL: Homology modelling of protein structures and complexes. *Nucleic Acids Res.* **46**, W296–W303 (2018).
61. B. Watzer *et al*., The signal transduction protein PII controls ammonium, nitrate and urea uptake in cyanobacteria. *Front. Microbiol.* **10**, 1428 (2019).
62. S. Klähn *et al*., The sRNA NsiR4 is involved in nitrogen assimilation control in cyanobacteria by targeting glutamine synthetase inactivating factor IF7. *Proc. Natl. Acad. Sci. U.S.A.* **112**, E6243–E6252 (2015).
63. M. García-Domínguez, J. C. Reyes, F. J. Florencio, NtcA represses transcription of *gifA* and *gifB*, genes that encode inhibitors of glutamine synthetase type I from *Synechocystis* sp. PCC 6803. *Mol. Microbiol.* **35**, 1192–1201 (2000).
64. N. Dolganov, A. R. Grossman, A polypeptide with similarity to phycocyanin α-subunit phycocyanobilin lyase involved in degradation of phycobilisomes. *J. Bacteriol.* **181**, 610–617 (1999).
65. B. Schwanhäusser *et al*., Global quantification of mammalian gene expression control. *Nature* **473**, 337–342 (2011).
66. Y. Wu, Q. Li, X.-Z. Chen, Detecting protein-protein interactions by Far western blotting. *Nat. Protoc.* **2**, 3278–3284 (2007).
67. H. Kirst, C. Formighieri, A. Melis, Maximizing photosynthetic efficiency and culture productivity in cyanobacteria upon minimizing the phycobilisome light-harvesting antenna size. *Biochim. Biophys. Acta* **1837**, 1653–1664 (2014).
68. P.-P. Hu *et al*., The role of lyases, NblA and NblB proteins and bilin chromophore transfer in restructuring the cyanobacterial light-harvesting complex‡. *Plant J.* **102**, 529–540 (2020).
69. S. Boussiba, A. E. Richmond, C-phycocyanin as a storage protein in the blue-green alga Spirulina platensis. *Arch. Microbiol.* **125**, 143–147 (1980).
70. E. Sendersky *et al*., The proteolysis adaptor, NblA, is essential for degradation of the core pigment of the cyanobacterial light-harvesting complex. *Plant J.* **83**, 845–852 (2015).
71. M. Levi, E. Sendersky, R. Schwarz, Decomposition of cyanobacterial light harvesting complexes: NblA-dependent role of the bilin lyase homolog NblB. *Plant J.* **94**, 813–821 (2018).
72. H. Sato, T. Fujimori, K. Sonoike, sll1961 is a novel regulator of phycobilisome degradation during nitrogen starvation in the cyanobacterium Synechocystis sp. PCC 6803. *FEBS Lett.* **582**, 1093–1096 (2008).
73. O. Cheregi, C. Funk, Regulation of the *scp* genes in the cyanobacterium *Synechocystis* sp. PCC 6803 — What is new? *Molecules* **20**, 14621–14637 (2015).
74. J. Komenda, R. Sobotka, Cyanobacterial high-light-inducible proteins–Protectors of chlorophyll-protein synthesis and assembly. *Biochim. Biophys. Acta* **1857**, 288–295 (2016).
75. G. Kufryk *et al*., Association of small CAB-like proteins (SCPs) of *Synechocystis* sp. PCC 6803 with photosystem II. *Photosynth. Res.* **95**, 135–145 (2008).
76. A. Baier, W. Winkler, T. Korte, W. Lockau, A. Karradt, Degradation of phycobilisomes in *Synechocystis* sp. PCC6803: Evidence for essential formation of an NblA1/NblA2 heterodimer and its codegradation by A Clp protease complex. *J. Biol. Chem.* **289**, 11755–11766 (2014).
77. D. Trautmann, B. Voss, A. Wilde, S. Al-Babili, W. R. Hess, Microevolution in cyanobacteria: Re-sequencing a motile substrain of *Synechocystis* sp. PCC 6803. *DNA Res.* **19**, 435–448 (2012).
78. H. M. Beyer *et al*., AQUA cloning: A versatile and simple enzyme-free cloning approach. *PLoS One* **10**, e0137652 (2015).
79. I. Scholz, S. J. Lange, S. Hein, W. R. Hess, R. Backofen, CRISPR-Cas systems in the cyanobacterium *Synechocystis* sp. PCC6803 exhibit distinct processing pathways involving at least two Cas6 and a Cmr2 protein. *PLoS One* **8**, e56470 (2013).
80. M. Li *et al*., Detection and characterization of a mycobacterial L-arabinofuranose ABC transporter identified with a rapid lipoproteomics protocol. *Cell Chem. Biol.* **26**, 852–862.e6 (2019).
81. T. Fujisawa *et al*., CyanoBase: a large-scale update on its 20th anniversary. *Nucleic Acids Res.* **45**, D551–D554 (2017).
82. Y. Perez-Riverol *et al*., The PRIDE database and related tools and resources in 2019: Improving support for quantification data. *Nucleic Acids Res.* **47**, D442–D450 (2019).
83. J. Cox *et al*., Accurate proteome-wide label-free quantification by delayed normalization and maximal peptide ratio extraction, termed MaxLFQ. *Mol. Cell. Proteomics* **13**, 2513–2526 (2014).
84. S. Tyanova *et al*., The Perseus computational platform for comprehensive analysis of (prote)omics data. *Nat. Methods* **13**, 731–740 (2016).
85. V. G. Tusher, R. Tibshirani, G. Chu, Significance analysis of microarrays applied to the ionizing radiation response. *Proc. Natl. Acad. Sci. U.S.A.* **98**, 5116–5121 (2001).
86. A. A. Arteni, G. Ajlani, E. J. Boekema, Structural organisation of phycobilisomes from *Synechocystis* sp. strain PCC6803 and their interaction with the membrane. *Biochim. Biophys. Acta* **1787**, 272–279 (2009).
87. E. Sendersky, R. Lahmi, J. Shaltiel, A. Perelman, R. Schwarz, NblC, a novel component required for pigment degradation during starvation in Synechococcus PCC 7942. *Mol. Microbiol.* **58**, 659–668 (2005).
88. L. G. van Waasbergen, N. Dolganov, A. R. Grossman, *nblS*, a gene involved in controlling photosynthesis-related gene expression during high light and nutrient stress in *Synechococcus elongatus* PCC 7942. *J. Bacteriol.* **184**, 2481–2490 (2002).
89. H. Kato *et al*., Interactions between histidine kinase NblS and the response regulators RpaB and SrrA are involved in the bleaching process of the cyanobacterium *Synechococcus elongatus* PCC 7942. *Plant Cell Physiol.* **52**, 2115–2122 (2011).